Ain Shams Engineering Journal xxx (xxxx) xxx

Contents lists available at ScienceDirect

Ain Shams Engineering Journal

journal homepage: www.sciencedirect.com

Full Length Article

Solar radiation and Lorentz force effects on Reiner-Rivlin nanofluid flow over a spinning disk with activation energy

Refat Ullah Jan [a], Ikram Ullah [b], Mohammad Mahtab Alam [c], Ali Hasan Ali [d,e,f,*]

[a] Islamia College Peshawar (Chartered University), KP 25000, Pakistan
[b] Department of Natural Sciences and Humanities, University of Engineering and Technology, Mardan 23200, Pakistan
[c] Department of Basic Medical Sciences, College of Applied Medical Science, King Khalid University, Abha 61421, Saudi Arabia
[d] Department of Business Management, Al-imam University College, Balad 34011, Iraq
[e] Institute of Mathematics, University of Debrecen, Pf. 400, H-4002 Debrecen, Hungary
[f] Technical Engineering College, Al-Ayen University, Dhi Qar 64001, Iraq

ARTICLE INFO

Keywords:
Entropy optimization
Exothermic/Endothermic reaction
Electric and Magnetic fields
Reiner-Revilin model
Joule heating
Activation energy

ABSTRACT

The enhancement of thermal efficiency in energy conversion processes holds great importance in numerous sectors. The addition of nanoparticles into working fluid helps in the attainment of improved thermal efficiency. Hence, the main objective of the present study is to examine the irreversibility of the flow of magnetized Reiner Rivlin nano-fluid over a stretchable rotating disk. The electrically conducted fluid takes into account in the presence of the induced electric field. The energy expression is characterized by exothermic or endothermic reactions with activation energy, radiation, Joule heating, dissipation effects and these phenomena are uniqueness of the current work. The disk surface is subjected to slip factor and suction/injection conditions. Impacts of random and thermophoresis diffusions are considered and investigated. The entropy rate is also incorporated. The system of ordinary differential equations (ODEs) is converted through the appropriate selection of variables. The ND-solve technique is utilized to approximate solutions. The physical explanation of the flow variables concerning velocity, thermal field and entropy optimization is provided. The computational results pertaining to Sherwood number, skin friction, and temperature gradient are discussed. Enhanced entropy generation occurs as the numeric values of the electric parameter, radiation parameter and Brinkman number increase. Therefore, motivated by the above practical application to attempt the present study.

1. Introduction

Nanomaterials has a variety of applications in many areas, including cooling towers, tumor therapy, microelectronics cooling, industrial cooling, imaging, heating of home appliances, development of new types of fuels, nanotechnology is used in human lives because of its importance and utilization in many sectors like in electronics, biomedical science, cancer treatment, agriculture, and medical sciences (nano robots are injected into the blood stream for recovery and repairing processes) [1]. Improvement of cutting-edge performance of isolated thermal systems for thermal carriage has become increasingly popular in recent years. It is due to its numerous uses in paper making industry, medical equipment, medicine production, heat exchangers, thermal power stations, thermal transport, microelectronics, and some relevant other fields. There are several methods for improving the efficiency of heat transfer of base liquid (air, water, kerosene oil, propylene and ethylene glycols) etc. Thermal heat transfer can also be improved by enhancing the heat transmission of the base liquid (working materials).

For this nanoparticles can be inserted to improve thermal conductivity of base liquids [2]. Nano sheets, nanowires, nanotubes, nanocones, nan-rods, nanoparticles, and nanofluids such as ethyl-glycol, oil, and water are examples of nanoscale materials. Drug delivery, protein engineering, cancer diagnostics and treatment, photodynamic treatment, biotherapy, shedding new light on cells, molecular motors such as kinesis surgery, and neuro electronic interfaces are just a few of the applications for nanofluids [3]. Choi and Eastman explained how nanoparticles distributed in a base liquid can be used in various thermal frameworks to improve the rate of heat exchange [4]. In the past few decades, nanoparticles have been utilized as an attractive agent in the production of fluids to improve heat transfer in automation technology [5]. The different applications and properties of nanofluid were

* Corresponding author.
E-mail address: ali.hasan@science.unideb.hu (A.H. Ali).

https://doi.org/10.1016/j.asej.2024.103063
Received 12 March 2024; Received in revised form 9 July 2024; Accepted 7 September 2024

Nomenclature

$u,\ v, w\left(ms^{-1}\right)$	Velocity components
L	Diffusion variable
δ_{ij}	Kronecker symbol
μ_c	Coefficient of cross viscosity
$T_\infty(K)$	Ambient temperature
$T(K)$	Fluid temperature
M	Magnetic parameter
C_w	Wall concentrations
τ_{ij}	Cauchy stress tensor
Ec	Eckert number
$k_f\left(kgmk^{-1}s^{-3}\right)$	Thermal conductivity
$\nu_f\left(m^2s^{-1}\right)$	Kinematic viscosity
k_r^2	Rate of reaction
B_T	Biot number due to temperature.
Re_r	Local Reynolds number
σ^*	Stephan-Boltzamnn constant
Nu_r	Nusselt number
$f'(\eta)$	Dimensionless radial velocity
(ρc_p)	Fluid heat capacity
Sh_r	Sherwood number
D_B	Brownian motion parameter
A	Stretching variable
Rd	Radiation variable
E_a	Activation energy
γ	Chemical reaction variable
α_1	Temperature difference variable
h_c	Coefficient of mass transfer
E_1	Electric parameter
Br	Brinkman number
Nt	Thermophoresis variable
$r,\ \varphi, z(m)$	Cylindrical coordinates
L_1	Velocity slip factor
$C_{f,r}$	Coefficient of Skin friction
j_w	Mass flux
$q_w\left(kgs^{-3}\right)$	Heat flux
λ_1	Exothermic reaction parameter
$p(pa)$	Pressure
c_p	Specific heat
μ_f	Dynamic viscosity
e_{ij}	Deformation rate tensor
$T_w(K)$	Wall temperature
$k^*\left(m^{-1}\right)$	Coefficient of mean absorption
B_c	Biot number due to concentration.
D_T	Thermophoresis coefficient
$\rho_f\left(kgm^{-3}\right)$	Density
β	Reiner-Rivlin fluid parameter
Pr	Prandtl number
Sc	Schmidt number
α_2	Concentration difference variable
$C_{m,r}$	Moment coefficient
u_w	Stretching velocity
σ_1	Reaction parameter
N_G	Rate of entropy generation
Nb	Brownian diffusion parameter
h_f	Coefficient of heat transfer
δ	Temperature ratio parameter
β_1	Suction/injection parameter

discovered by many others researchers by taking the novel approach and tried something new [6–28]. It is also shown that spherical nanoparticles contribute less heat exchange, but platelet nanoparticles deliver higher heat transfer [29]. Ullah et al [30] investigated the use of an infinite porous disk to communicate the Marangoni convection flow of hybrid nanomaterials.

In 1889, a Swedish scientist named Arrhenius coined the term activation energy, which can be defined as the Minimum quantity of energy essential to activate a chemical process. The Arrhenius equation can be used to calculate the quantity of activation energy [31]. The minimal energy acquired by the atoms or molecules to activate the chemical reaction is denoted by E_a, which is measured in KJ/mol. Bestman [32] published the earliest paper on activation energy in binary chemical reactions. Awad et al. [33] investigated the effects of activation energy and binary chemical process in a viscous rotating flow. Ullah et al. [34] examined numerically the flow of second-grade nanoliquid with the Arrhenius activation energy and binary chemical reaction in a spongy media. Examples of activation energy and chemical reactions comprise of thermal oil recovery, food processing, chemical energy, geothermal engineering, water emulsion and nuclear reactors [35]. The implications of activation energy in melting conditions on nanofluid flow are investigated theoretically [36]. Ullah et al. [37] investigated the combined heat source and features of zero mass flux on magnetic nanofluid flow by radial disk with the use of activation energy.

Entropy is a term that refers to the unpredictability or disorder of a system or environment. The relation of reversible heat to temperature is also used to calculate entropy. The performance of thermal machines such as air conditioners, heat pumps, and energy plants is measured due to entropy generation. Bejan [38] for the first time addressed the entropy generation problem. Alkanhal et al. [39] investigate entropy generation for magnetohydrodynamic flow of nanofluids with convective heat transfer. Li et al. [40] used helical twisted tapes to demonstrate entropy analysis on nanofluids with convective heat transfer. The generation of entropy can be used as a criteria for evaluating the performance of engineering devices [41]. Dormohammadi et al. [42] investigated the effects of entropy generation optimization on nanomaterial convective flow with heat flux. Rashidi et al. [43] investigated the generation of entropy in 3rd-grade fluid. K. Loganathan et al. [3] used the CCHF model to investigate the impact of 3rd-grade nanofluid flow across a convective surface of inclined magnetic field impacts on entropy formation of 3rd-grade nanofluid across the convective surface. Micro polar nanofluid free convection and entropy generation are achieved using an inclined I-shaped cage with two heated cylinders [44].

Fortified from of all the above theoretical and mathematical work discussed in literature regarding nanofluid flow, heat transfer exploration and entropy analysis to a diverse geometry. Our objective here is to consider the significances of nanofluid flow, activation energy with exothermic/endothermic reaction and entropy generation in the presence of radiation, Joule heating and Lorentz force. The novelty structure of this proposed efforts are as follows.

- To model the entropy analysis in Reiner-Rivlin nanofluid past a rotating disk.
- An Exothermic/endothermic reaction along with activation energy which start the chemical reaction is taken detail analysis of heat transfer.
- The slip factor and convective conditions are imposed at the boundary.
- To see the significant changes in velocity gradient and rate of heat transfer against involve parameters.

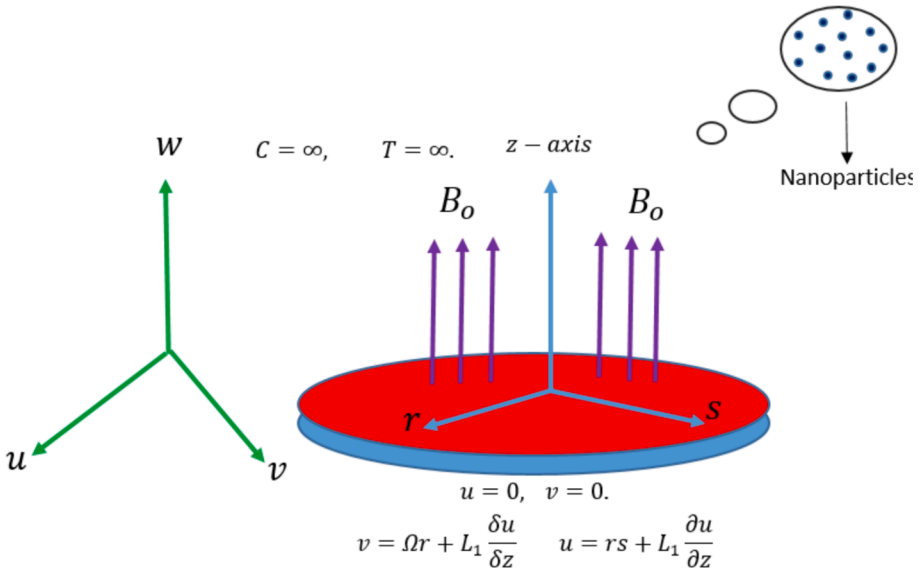

Fig. 1. Flow configuration.

- To inspect the variations in thermal analysis in the presence of exothermic reaction.
- To show the influence of the rate of heat energy with variation in various parameters.
- To study the physical behavior of entropy generation through rise in different influential variables.

System of ordinary differential equation have been obtained through applying suitable transformation technique. The Modeled system have been attempted through NDSolve method. Various variables on concentration, and temperature and entropy optimization are entertained through graphs and tables. The remarkable properties of this theoretical study have potential applications in various fields, including material science, purification technologies, optics, electricity, aerospace industry, and beyond. Particularly in the aerospace sector, this assistance can be instrumental in reducing weight, achieving satellite weight reduction, providing lightning protection for aircraft, and more.

2. Mathematical modeling

In this section the 3D steady flow of Reiner-Rivlin nanofluid by a stretchable rotating disk is considered. The disk is rotating with velocity (Ωr). Heat equation modeled through dissipations, radiation, random and thermophoresis diffusion, are considered. Electric and magnetic fields are added for further inspection. To study irreversibility analysis, the 1st and 2nd law of thermodynamics are implemented. The reaction rate is also taken into account. Cylindrical coordinates (r, φ, z) are used to model the governing equation. Let $u_w = rs$ is considered as stretching velocity with stretching rate constant $(s > 0)$. Furthermore, suction/injection and slip effects are included for heat transfer and flow investigation. In light of the preceding considerations, the flow governing expressions governing expressions [45] are: (See Fig. 1)

$$\tau_{ij} = \mu_f e_{ij} - p\delta_{ij} + \mu_c e_{ik} e_{kj} e_{jj}. \tag{1}$$

In the above equation the p indicates pressure, μ_f dynamic velocity, e_{ij} the deformation rate tensor and δ_{ij} the kronecker delta.

$$\frac{\partial u}{\partial r} + \frac{u}{r} + \frac{\partial w}{\partial z} = 0, \tag{2}$$

$$u\frac{\partial u}{\partial r} - \frac{v^2}{r} + w\frac{\partial u}{\partial z} = \nu_f \frac{\partial^2 u}{\partial z^2} + \frac{\mu_c}{\rho_f}\left(\begin{array}{l} u\frac{\partial u \partial^2 u}{\partial z \partial r \partial z} + 2\frac{\partial u \partial^2 u}{\partial r \partial z^2} + 2\frac{\partial w \partial^2 u}{\partial z \partial z^2} + \\ \frac{\partial^2 v}{\partial z^2}\left(\frac{\partial u}{\partial r} - \frac{v}{r}\right) + \frac{\partial v}{\partial z}\left(\frac{\partial^2 v}{\partial r \partial z} - \frac{1}{r}\frac{\partial v}{\partial z}\right) + \\ 2\frac{\partial u \partial^2 w}{\partial z \partial z^2} + \frac{1}{r}\left(\left(\frac{\partial u}{\partial z}\right)^2 - \left(\frac{\partial v}{\partial z}\right)^2\right) \end{array}\right) + \frac{\delta}{\rho_f}(E_o B_o - B_o^2 v) \tag{3}$$

$$u\frac{\partial u}{\partial r} + \frac{uv}{r} + w\frac{\partial u}{\partial z} = \nu_f \frac{\partial^2 v}{\partial z^2} + \frac{\mu_c}{\rho_f}\left(\begin{array}{l} \frac{\partial v \partial^2 u}{\partial z \partial r \partial z} + 2\frac{\partial u \partial^2 u}{\partial r \partial z^2} + 2\frac{\partial u \partial v}{\partial z^2 \partial z} + \\ \frac{\partial^2 u}{\partial z^2}\left(\frac{\partial v}{\partial r} - \frac{v}{r}\right) + \frac{\partial u}{\partial z}\left(\frac{\partial^2 v}{\partial r \partial z} - \frac{1}{r}\frac{\partial v}{\partial z}\right) + \\ 2\frac{u\partial^2 v}{r\partial z^2} + 2\frac{\partial^2 u}{r\partial z^2}\left(\left(\frac{\partial u}{\partial z}\right)^2 - \left(\frac{\partial v}{\partial z}\right)^2\right) \end{array}\right) + \frac{\delta}{\rho_f}(E_o B_o - B_o v) \tag{4}$$

$$\left.\begin{array}{l} u\frac{\partial T}{\partial r} + w\frac{\partial T}{\partial z} = \frac{k_f}{(\rho c_p)_f}\left(1 + \frac{16\sigma^* T_\infty^3}{3k_f k^*}\right)\frac{\partial^2 T}{\partial z^2} + \tau\left(D_B \frac{\partial T \partial C}{\partial z \partial z} + \frac{D_T}{T_\infty}\left(\frac{\partial T}{\partial z}\right)^2\right) \\ + \frac{\mu_f}{(\rho c_p)_f}\left(\left(\frac{\partial u}{\partial z}\right)^2 + \left(\frac{\partial v}{\partial z}\right)^2\right) + \beta_1 k_r^2 (C - C_\infty)\left(\frac{T}{T_\infty}\right)^m \exp\left(\frac{E_a}{\kappa T}\right), \\ + \frac{\mu_f}{(\rho c_p)_f}\left(\begin{array}{l} \frac{\partial w}{\partial z}\left(\frac{\partial v}{\partial z}\right)^2 + \frac{\partial u \partial v \partial v}{\partial z \partial z \partial r} - \frac{v \partial u \partial v}{r \partial z \partial z} + 2\frac{u}{r}\left(\frac{\partial v}{\partial z}\right)^2 \\ 2\frac{\partial u \partial u}{\partial z \partial r}\left(\frac{\partial u}{\partial z} + \frac{\partial w}{\partial z}\right) + \left(\frac{\partial u}{\partial z} + \frac{\partial w}{\partial z}\right)\left(\frac{\partial v}{\partial r} - \frac{v}{r}\right)\frac{\partial v}{\partial z} \\ 2\frac{\partial u \partial w}{\partial z \partial z}\left(\frac{\partial u}{\partial z} + \frac{\partial w}{\partial z}\right) + \frac{\partial v \partial u}{\partial z \partial z}\left(\frac{\partial v}{\partial r} - \frac{v}{r}\right) + 2\frac{\partial w}{\partial z}\left(\frac{\partial v}{\partial z}\right)^2 \end{array}\right) + \\ \frac{\delta_f}{(\rho c_p)_f}\{(u^2 + v^2)\beta_0^2 - 2E_0^2\}, \end{array}\right\} \tag{5}$$

$$u\frac{\partial C}{\partial r} + w\frac{\partial C}{\partial z} = D_B \frac{\partial^2 C}{\partial z^2} + \frac{D_T}{T_\infty}\frac{\partial^2 T}{\partial z^2} - k_r^2 (C - C_\infty)\left(\frac{T}{T_\infty}\right)^m \exp\left(\frac{-E_a}{\kappa T}\right), \tag{6}$$

with conditions

$$\left.\begin{aligned} u=sr+L_1\frac{\partial u}{\partial z}, \qquad & v=\Omega r+L_1\frac{\partial u}{\partial z},\ w=-w_0,\\ k\frac{\partial T}{\partial z}=-h_f(T_f-T),\ -D_B\frac{\partial C}{\partial z}=h_c(C_f-C),\ & at\ z=0,\\ u\to 0,\ v\to 0, C\to C_\infty, T\to T_\infty,\ & as\ z\to\infty. \end{aligned}\right\} \tag{7}$$

Utilizing

$$\left.\begin{aligned} u=r\Omega f'(\eta),\quad w=2\sqrt{\Omega\nu_f}f(\eta),\ v=r\Omega g(\eta),\\ \theta(\eta)=\frac{(T-T_\infty)}{(T_f-T_\infty)},\ \phi(\eta)=\frac{(C-C_\infty)}{(C_f-C_\infty)},\ \eta=\sqrt{\frac{\Omega}{\nu_f}}z, \end{aligned}\right\} \tag{8}$$

Eq. (1) is satisfied identically whereas other expressions are

$$f'''-f'^2+2ff''+g^2+\beta(ff''^2-2f'f'''-g'^2)+M(E_1-f')=0, \tag{9}$$

$$g''-2fg'+2f'g+2b(f''g'+f'g'')+M(E_1-g)=0, \tag{10}$$

$$\left.\begin{aligned} (1+Rd)\theta''+Prf\theta'+Br(1-3\beta f')(f'^2+g'^2)+PrNb\theta'\phi'+PrNt\theta'^2\\ +\lambda_1\sigma_1(1+\delta\theta)^m\exp\left(-\frac{E_a}{(1+\delta\theta)}\right)+MBr(f'^2+g^2-E_1^2)=0, \end{aligned}\right\} \tag{11}$$

$$\phi''+Scf\phi'+\frac{Nt}{Nb}\theta''-Sc\sigma_1(1+\delta\theta)^m\exp\left(-\frac{E_a}{(1+\delta\theta)}\right)=0, \tag{12}$$

$$\left.\begin{aligned} f'(0)=\gamma+\gamma_s f''(0), \qquad & f(0)=\beta_1,\ g(0)=1+\gamma_s g'(0),\\ \theta'(0)=-B_T(1-\theta(0)),\ \phi'(0)=-B_c(1-\phi(0)),\ & \\ f'(\infty)=\theta(\infty)=\phi(\infty)=0. & \end{aligned}\right\} \tag{13}$$

Here the dimensionless parameter are defined as

$$\left.\begin{aligned} Rd=\frac{16\sigma^*T_\infty^3}{3k_fk^*},\ \beta=\frac{\mu_c\Omega}{\mu_f},\ \gamma=\frac{s}{\Omega},\ Ec=\frac{u_w^2}{c_p(T_f-T_\infty)},\ Nt=\frac{\tau D_T(T_f-T_\infty)}{T_\infty\nu_f}\\ Pr=\frac{\mu_f c_p}{k_f},\ Nb=\frac{\tau D_B(C_f-C_\infty)}{\nu_f},\ Br=PrEc,\ Sc=\frac{\nu_f}{D_B},\ \beta_2=\frac{w_o}{\sqrt{2\Omega\nu_f}},\\ E_1=\frac{E_0}{\gamma\Omega B_0},\ M=\frac{\sigma B_o^2}{\rho_f\Omega},\ \lambda_1=\frac{B_1C_\infty}{(\rho c_p)_f(T_f-T_\infty)},\ \delta=\frac{T_f-T_\infty}{T_\infty},\ E=\frac{E_a}{k_fT_\infty},\\ \sigma_1=\frac{K_r^2}{s},\ B_c=\frac{h_f}{D_b}\sqrt{\frac{\nu_f}{2\Omega}},\ B_T=\frac{h_c}{k_f}\sqrt{\frac{\nu_f}{2\Omega}},\ \mathrm{Re}=\frac{r^2\Omega}{\nu_f},\ \gamma_S=Lu_f\sqrt{\frac{2\Omega}{\nu_f}}. \end{aligned}\right\} \tag{14}$$

In the above equations, Eq. (2) is based on the conservation of mass as continuity equation. Eq. (3) shows momentum equation, its L.H.S shows internal forces, where the 1st term in the R.H.S is surface force and 2nd term as body forces (induced electric and magnetic force), the 5th equation is energy equation, the L.H.S is total internal energy, whereas, 1st term in R.H.S is thermal radiation, 2nd term is Fourier's law of heat flux, 3rd term is viscous dissipation, 4th term is exothermic, endothermic energy. There is activation energy in the 6th equation. Eq. (7) has velocity slip, angular velocity, convective boundary condition for heat and mass diffusion.

Where *Rd* radiation parameter, β suction /injection parameter, γ stretching variable, Ecket number *Ec*, *Nt* thermophoretic variable, *Pr* Prandtl number, *Nb* Brownian diffusion variable,*Br* Brinkman number, *Sc* Schmidt number, β_2 suction number, E_1 the electric parameter, *M* magnetic parameter, λ_1 exothermic reaction parameter, δ temperature ratio parameter, T_f temperature of heated fluid, β_0 is the strength of the magnetic field applied, *L* diffusion parameter, γ_s slip parameter, σ_1 is the reaction parameter, B_c and B_T denotes Biot number due to concentration and and temperature respectively.

3. Entropy modeling

Mathematical expression for entropy is

$$\left.\begin{aligned} S_G=\frac{k_f}{T_\infty^2}\left(1+\frac{16\sigma^*T_\infty^3}{3k_fk^*}\right)\left(\frac{\partial T}{\partial z}\right)^2+\frac{\mu_f}{T_\infty}\left(\left(\frac{\partial u}{\partial z}\right)^2+\left(\frac{\partial v}{\partial z}\right)^2\right)\\ +\frac{\mu_f}{T_\infty}\left(\begin{array}{c} \frac{\partial w}{\partial z}\left(\frac{\partial v}{\partial z}\right)^2+\frac{\partial v\partial u\partial v}{\partial z\partial z\partial z}-\frac{v\partial u\partial v}{r\partial z\partial z}2\frac{u}{r}\left(\frac{\partial v}{\partial z}\right)^2\\ 2\frac{\partial u\partial u}{\partial z\partial r}\left(\frac{\partial w}{\partial z}+\frac{\partial u}{\partial z}\right)+\left(\frac{\partial w}{\partial z}+\frac{\partial u}{\partial z}\right)\left(\frac{\partial w}{\partial z}-\frac{v}{r}\right)\frac{\partial v}{\partial z}\\ +2\frac{\partial w\partial u}{\partial z\partial z}\left(\frac{\partial w}{\partial z}+\frac{\partial u}{\partial z}\right)+\frac{\partial u\partial v}{\partial z\partial z}\left(\frac{\partial v}{\partial z}-\frac{v}{r}\right)+2\frac{\partial w}{\partial z}\left(\frac{\partial v}{\partial z}\right)^2\\ \frac{R_D}{T_\infty}\left(\frac{\partial C\partial T}{\partial z\partial z}\right)+\frac{R_D}{T_\infty}\left(\frac{\partial C}{\partial z}\right)^2. \end{array}\right) \end{aligned}\right\} \tag{15}$$

Using eq. (8), the above expression reduces to

$$\left.\begin{aligned} S_G=\alpha_1(1+Rd)\theta'^2+Br(1-3\beta f')(f''^2+g'^2)+\frac{\alpha_1}{\alpha_2}g\phi'^2+L\theta'\phi'+\\ L\frac{\alpha_1}{\alpha_2}\phi'^2+M(f'^2+g^2-E_1^2). \end{aligned}\right\} \tag{16}$$

The dimensionless variables are

$$\left.\begin{aligned} S_G=\frac{S_G\nu_fT_\infty}{k_f\Omega(T_f-T_\infty)},\ L=\frac{R_D(C_f-C_\infty)\nu_fT_\infty}{k_f},\ \alpha_1=\frac{(T_f-T_\infty)}{T_\infty},\ \alpha_2\\ =\frac{(C_f-C_\infty)}{C_\infty}. \end{aligned}\right\} \tag{17}$$

4. Physical quantities

The physical quantities i.e. moment coefficient is defined as

$$C_{m,r}=\frac{T_r}{\rho_f\Omega^2r^5}, \tag{18}$$

where T_r specifies torque of rotating disk and is given by

$$T_r=r_0\tau_{z\phi}2\pi r^2dr=\frac{\pi}{2}\rho_f\Omega\sqrt{\nu_f\Omega}(1-2\beta A)r^4g'(0), \tag{19}$$

$$\mathrm{Re}_r^{\frac{1}{2}}C_{m,r}=\tfrac{\pi}{2}(1-2A\beta)g'(0). \tag{20}$$

Table 1
Comparative analysis of present results, when $M = E_1 = \gamma = \beta_1 = \gamma_s = L_1 = \delta = B_T = B_C = \lambda_1 = 0, \beta = 0.2$, Nt = 0.5, s = 0.1, Pr = 3, Rd = 0.1, Nb = 0.5, Br = 0.5, = 0, $m_1 = 2$, $E_a = 1$, Sc = 3, $\sigma_1 = 0.2$, = 1, with the Sadiq and Hayat [3].

Sadiq and Hayat [34]					Present result	
Nb	*Nt*	*Sc*	Nu_r	Sh_r	Nu_r	Sh_r
0.6	0.5	0.5	0.156353	0.359172	0.156342	0.359201
0.8			0.121314	0.383214	0.121311	0.383232
1.2			0.091232	0.434652	0.091227	0.434644
0.6	0.2	0.5	0.137351	0.314951	0.137348	0,314,936
	0.6		0.118341	0.278961	0.118339	0.278923
	1.0		0.084591	0.257351	0.084588	0.257344
	0.5	0.5	0.234653	0.354950	0.234647	0.354946
		0.7	0.197563	0.393560	0.197571	0.393572
		0.9	0.156573	0.457571	0.156498	0.457562

Skin friction is expressed as

$$C_{f,r} = \frac{\tau_{zr}}{\rho_f (r\Omega)^2}, \tag{21}$$

the dimensionless form is

$$\mathrm{Re}_r^{\frac{1}{2}} C_{f,r} = f''(0)(1 - 2A\beta). \tag{22}$$

Nusselt and Sherwood numbers are defined as follow

$$Nu_r = \frac{rq_w}{k_f (T_w - T_\infty)}, Sh_r = \frac{rj_w}{D_\beta (C_w - C_\infty)}. \tag{23}$$

In dimensionless expression is

$$\mathrm{Re}_r^{-\frac{1}{2}} Sh_r = -\phi'(0), \mathrm{Re}_r^{-\frac{1}{2}} Nu_r = -(1 + Rd)\theta'(0), \tag{24}$$

the disk pumping efficiency is given by

$$Q = R_0 - 2\pi r dr(w(\infty)) = 2\Omega\sqrt{\nu_f \Omega}\pi R^2 f(\infty). \tag{25}$$

5. Method of solution and validation: —

The governing problem is modeled as non-linear system. Consequently, its exact solution is not possible to obtain. Therefore, an approximated solution can be obtained through different analytical and numerical techniques. Here in the current problem, NDSolve [46,47] based shooting technique is implemented to stimulate the results in tabular and graphical forms. This technique is stable unconditionally and attains exceptional accuracy, moreover it provides outstanding results in less CPU time and evade lengthy expressions. Table. 1 depicts the comparative scrutiny with Sadiq and Hayat [47]. It is observed that current and existing outcomes manifest good match.

6. Graphical results

Here main emphasis of this portion is to inspect the behavior of significant variables on temperature, entropy rate and concentration. Computational outcomes of Nusselt, Sherwood numbers and skin friction are explored in tabular form. The fixed values of the corresponding parameters are considered as $M = 0.5, \beta = 0.2, E_1 = 0.1, \gamma = 0.5, \gamma_s = 0.1$, Pr = 4, Rd = 0.1, Nt = 0.5, Nb = 0.5, Br = 0.5, $\lambda_1 = 0.001, \delta = 0$, $m_1 = 1$, $E_a = 1$, Sc = 3, $\sigma_1 = 3$, $B_T = 1$, $B_C = 0.2$.

6.1. Variation in temperature

Figs. 2 – 4 are designed for temperature against different variables. The fixed values of the concerning parameters are considered as $M = 0.5, \beta = 0.2, E_1 = 0.1, \gamma = 0.5, \gamma_s$, s = 0.1, Pr = 3, Rd = 0.1, Nt = 0.5, Nb = 0.5, Br = 0.5, $\lambda_1 = 0.001, \delta = 0.2$, $m_1 = 2$, $E_a = 1$, Sc = 3, $\sigma_1 = 0.2$, $B_T = 1$, $B_C = 0.2$. Behaviors of temperature δ is portrayed in Fig. 2a. Here it is investigated that larger value of temperature ratio parameter δ decay the temperature. Fig. 2b labels that for higher activation energy E_a the liquid temperature $\theta(\eta)$ improves. Physically, an enhancement in E_a correspond to increase in energetic nanoparticles possessing energies greater or equal to E_a, which improves the temperature. The variation in $\theta(\eta)$ against λ_1 is depicted in Fig. 3a, it indicates that temperature is higher for higher λ_1.In fact, higher λ_1 provides more heat to the

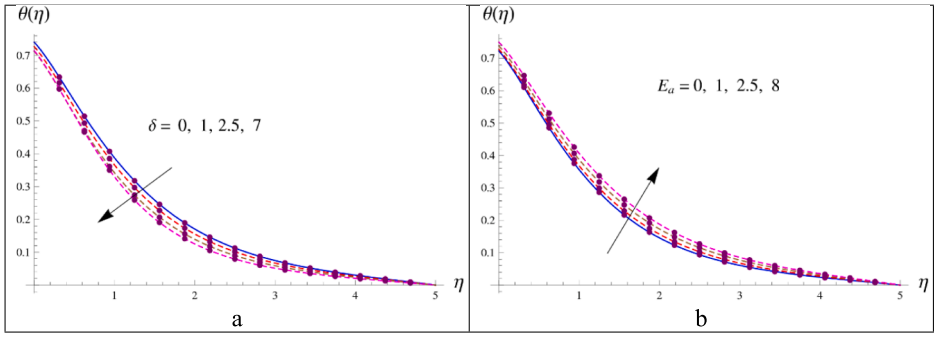

Fig. 2. (a, b) Temperature $\theta(\eta)$ for δ and E_a.

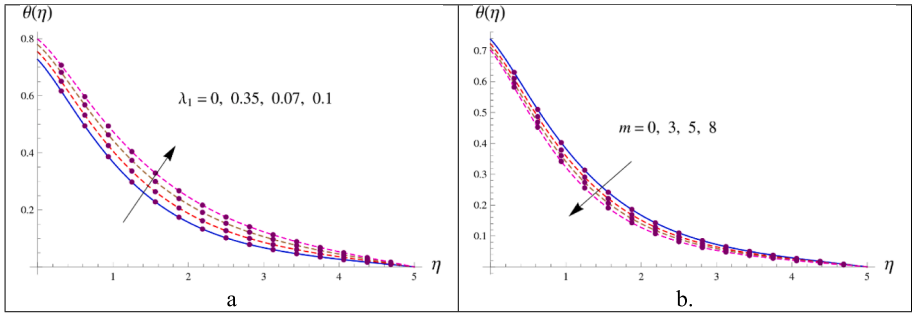

Fig. 3. (a, b) Temperature $\theta(\eta)$ for λ_1 and m.

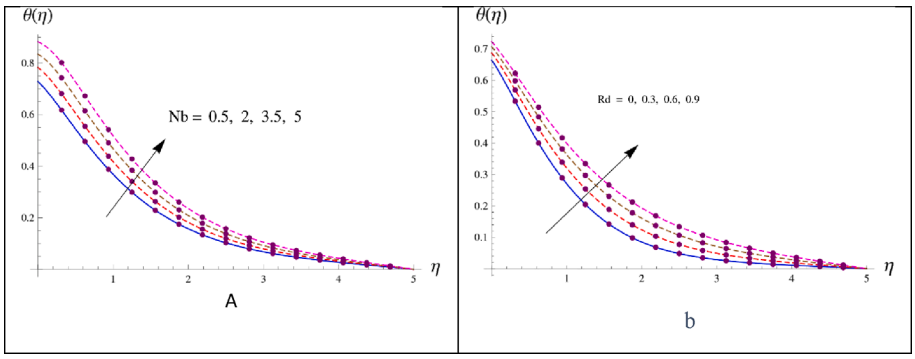

Fig. 4. (a, b) Temperature $\theta(\eta)$ for *Nb* and Rd.

operating liquid due to exothermic reaction. Thus $\theta(\eta)$ enhances. For higher values of fitted rate constant m a decreasing effect in liquid temperature is noticed, which is drawn in Fig. 3b. Features of $\theta(\eta)$ through variation in *Nb* is designed in Fig. 4a. Here temperature is significantly rises for large *Nb*. The rate of Brownian motion of nanoparticles increases in this case, and the consequent disorder in particle motion creates kinetic energy in nanoparticle and improves the thermal behavior of the liquid. The temperature variation via radiation parameter *Rd* is depicted in Fig. 4b. Physically, a reduction in the coefficient of mean absorption leads to a rise in thermal flux. As a result, temperature distribution is enhanced.

6.2. Variation in concentration

Figs. 5 and 6 are sketched to examine the behavior of concentration against numerous parameters with fixed values $M = 0.5, \beta = 0.2, E_1 = 0.1, \gamma = 0.5, \gamma_s = 0.1, \mathrm{Pr} = 4, \mathrm{Rd} = 0.1, \mathrm{Nt} = 0.5, \mathrm{Nb} = 0.5, \mathrm{Br} = 0.5,$ $\lambda_1 = 0.001, \delta = 0, \mathrm{m}_1 = 1, \mathrm{E}_a = 1, \mathrm{Sc} = 3, \sigma_1 = 3, \mathrm{B}_T = 1, B_C = 0.2$. It is depicted in Fig. 5a that with the increase in temperature ratio parameter, concentration of the fluid decreases, while the same decreasing effect of concentration is recorded with the enhancement in Brownian diffusion parameter (see Fig. 5b). Infact higher values Nb, speed up the collection between particles which gradually decays concentration. The boosting effect is noticed in concentration with increasing the thermophoresis variable, which can clearly be seen in Fig. 6a. Physically thermophoresis phenomenon corresponds to extraction of nanoparticles from hotter zone towards ambient materials. As a consequence, the thermophoretic force admit nanoparticles to carry heat from the surface to the working liquids and thus concentration enhanced. Where reaction parameter implies diminishing effect on concentration sown in Fig. 6b.

6.3. Variation entropy

Figs. 7 – 8 are drawn to investigate the entropy rate against different

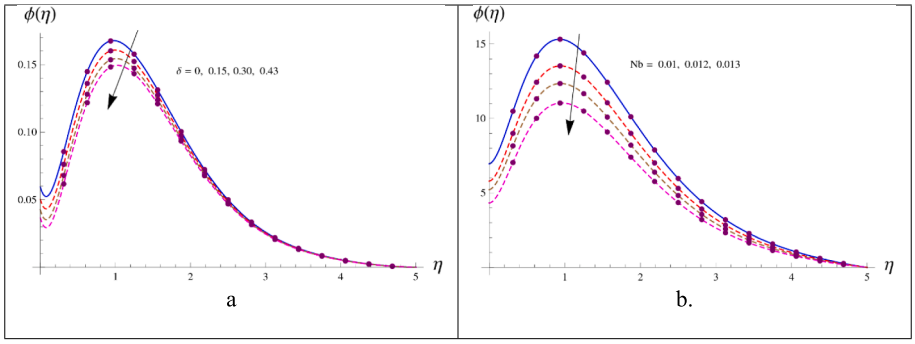

Fig. 5. (a, b). Concentration $\phi(\eta)$ for δ and *Nb*.

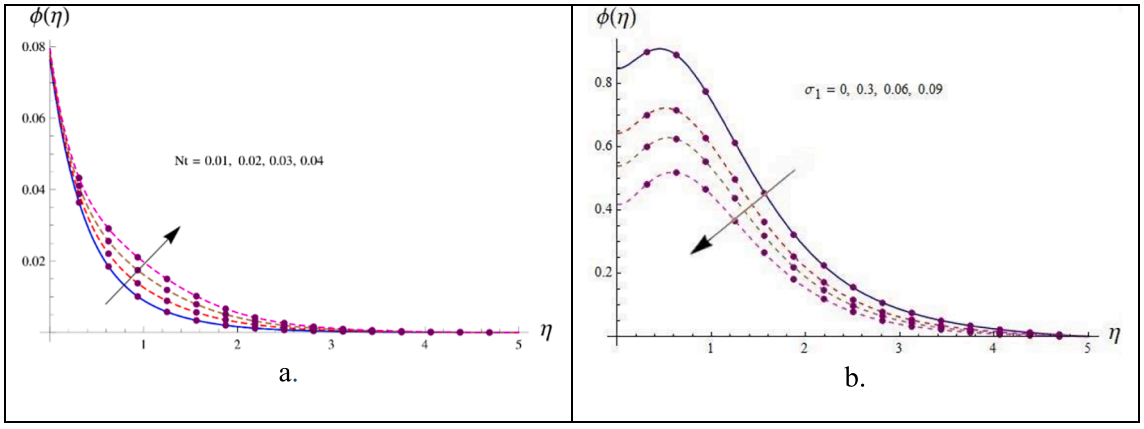

Fig. 6. (a, b). Concentration $\phi(\eta)$ for *Nt* and σ_1.

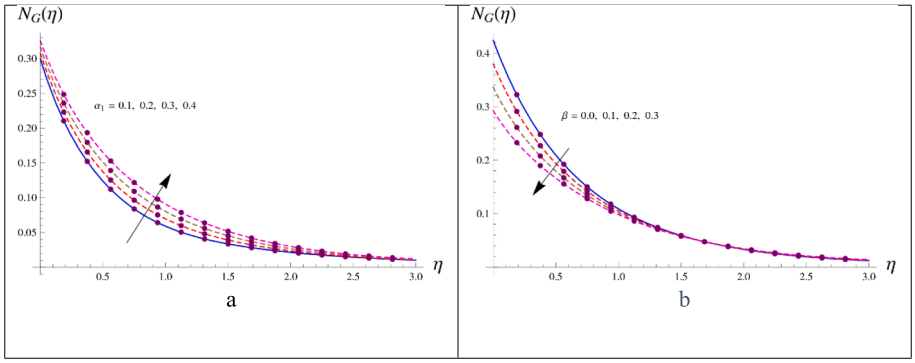

Fig. 7. (a, b) Entropy $N_G(\eta)$ for α_1 and β.

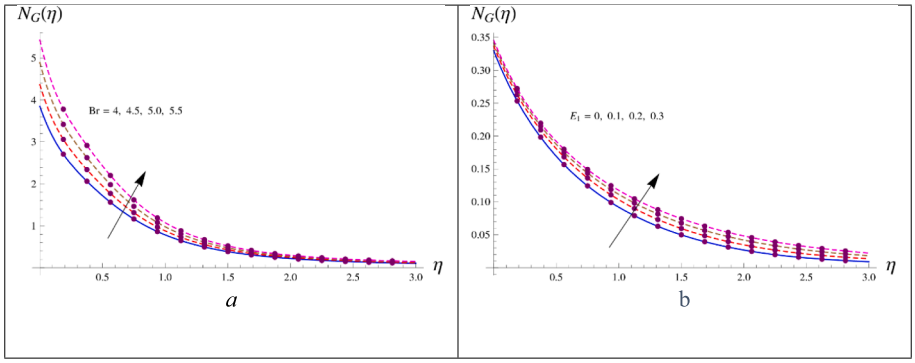

Fig. 8. (a, b) *Entropy* $N_G(\eta)$ *for Br and* E_1.

influencing parameters. Graphical interpretation of temperature difference variable against entropy rate is displayed in Fig. 7a. An enhancement is seen in entropy rate with the increase in temperature difference parameter. Through the enhancement in Reiner-Rivilin fluid parameter, a physical changed is observed in the entropy generation which can clearly be observed in Fig. 7b. Fig. 8a shows a physical description of the entropy rate as a function of Brinkman number (). A high Brinkman number indicates higher viscous force, which increases resistance among liquid particles. As a result, entropy generation is boosted up. Entropy generation has an increasing effect with increase in electric parameter which is displayed in Fig. 8b.

Table 2

Numerical results of $(\mathrm{R}_e^{-\frac{1}{2}}C_{f,r})$ for M, E_1, β, β_1, γ and γ_S.

M	E_1	β	β_1	γ	γ_s	$\mathrm{Re}_r^{-\frac{1}{2}}C_{fr}$
0.0	0.2	0.1	0.2	0.5	0.2	0.27675
0.3						0.27700
0.6						0.27906
0.2	0.0	0.1	0.2	0..5	0.2	0.29197
	0.2					0.27695
	0.4					0.25447
0.2	01	0.0	0.2	0.5	0.5	0.29141
		0.1				0.27695
		0,2				0.25922
0.2	0.1	0.5	0.0	0.5	0.5	0.17425
			0.2			0.27695
			0.4			0.40126
0.2	0.1	0.1	0.2	0.5	0.5	0.27695
				0.6		0.38786
				0.7		0.50119
0.2	0.1	0.1	0.2	0.5	0.0	0.29180
					0.2	0.27700
					0.4	0.24497

6.4. Engineering interest

The influence of numerous variables such as magnetic parameter M, the electric parameter E_1, Reiner- Rivilin fluid parameter β, suction/

Table 3

Numerical results of $(\mathrm{R}_e^{-\frac{1}{2}}Nu_r)$ for Rd, Br, E_a, λ_1, δ, Nt, Nb, Bt and E_1.

Rd	Br	E_1	λ_1	δ	Nt	Nb	Bt	E_1	$R_r^{-\frac{1}{2}}Nu_r$
0.0	0.5	01	0.001	0.2	0.5	0.2	01	0.2	0.32973
0.2									0.37172
0.4									0.41021
0.2	0.0	01	0.001	0.2	0.5	0.2	01	0.2	0.54000
	0.2								0.49554
	0.4								0.45091
0.2	01	01	0.001	0.2	0.5	0.2	01	0.2	0.42759
		02							0.42042
		03							0.41210
0.2	0.5		0.0	0.2	0.5	0.2	01	0.2	0.42927
			0.01						0.42195
			0.02						0.41491
0.2	0.5	01	0.01	0.0	0.5	0.2	01	0.2	0.42625
				0.2					0.42853
				0.4					0.43121
0.2	0.5	01	0.01	0.2	0.0	0.2	01	0.2	0.52983
					0.4				0.44721
					0.8				0.37681
0.2	0.5	01	0.01	0.2	0.5	0.1	01	0.2	0.43125
						0.3			0.42448
						0.6			0.41217
0.2	0.5	01	0.01	0.2	0.5	0.2	0.1	0.2	0.10516
							01		0.50157
							02		0.50256
0.2	0.5	01	0.01	0.2	0.5	0.2	01	0.0	0.41340
								0.1	0.42853
								0.3	0.43590

Table 4

Numerical results of $(R_e^{-\frac{1}{2}}Sh_r)$ for E_a,δ_1,δ, Bc,Nt and Nb.

E_a	σ_1	δ	$B\,c$	$N\,t$	Nb	$R_r^{-\frac{1}{2}}Sh_r$
01	0.9	0.2	0.2	0.5	0.2	0.13556
02						0.07333
03						0.01924
01	0.1	0.2	0.2	0.5	0.2	0.00497
	0.3					0.06304
	0.5					0.09643
01	0.9	0.0	0.2	0.5	0.2	0.12650
		0.3				0.13963
		0.6				0.14990
01	0.9	0.2	0.1	0.5	0.2	0.06876
			0.2			0.13556
			0.4			0.25025
01	0.9	0.2	0.2	0.0	0.2	0.17844
				0.4		0.13755
				0.6		0.13590
01	0.9	0.2	0.2	0.5	0.1	0.08080
					0.2	0.13556
					0.3	0.15144

injection parameter β_1, chemical reaction variable γ and slip parameter γ_s on skin friction coefficient $Re_r^{-\frac{1}{2}}C_{f,r}$ is shown in Table.2. For linger, E_1, β, and γ_s the skin friction coefficient begins to decline, while the opposite effect can clearly be observed via the enhancement in the parameters M, β_1 and γ. Table 3 illustrates the Nusselt number behavior for various influential physical parameters used in this study. Here Rd, δ, Bt and E_1 reveal an enhancing effect over the Nusselt number while Br, E_a, λ_1, Nt and Nb depicts reverse features. Table. 4 gives the numerical data of Sherwood number in the variations of different influential parameters. Here Sherwood number increases for δ_1 and δ whereas decays for E_a.

7. Concluding remarks

In this research article, the collective features of three dimensional Reiner-Rivilin nanofluid over a rotating disk is explored. Additionally, the flow system is modeled by the considering electrical and activation energies. The key themes are revealed as given below.

- Velocity $g(\eta)$ displays the opposite tendency for higher magnetic parameter M and electric parameter E_1.
- Thermal field is more dynamic over the increasing values of activation energy E_a, Brownian diffusion parameter Nb and radiation variable Rd.
- Concentration is productive up with improving values of activation energy E_a and thermophoresis parameter N_t, however opposite behavior is noticed for δ and N_b.
- Higher γ leads to additional drag force over the surface of the rotating disk.
- Nusselt number has an enhancing effect for the influential parameters Rd, δ, Bt and E_1.
- An amplification is noticed in Sherwood number for Biot number Bc and Brownian diffusion variable Nb.
- Entropy optimization is improved for the parameters temperature difference variable α_1, radiation Rd, Brinkman number Br and electric parameter E_1.
- The present analysis is only valid for incompressible viscous and electrically conducting fluid and these are the key limitations.

CRediT authorship contribution statement

Refat Ullah Jan: Formal analysis, Visualization, Writing – original draft, Conceptualization, Methodology. **Ikram Ullah:** Investigation, Supervision, Conceptualization, Writing – original draft. **Mohammad Mahtab Alam:** Visualization, Data curation, Writing – original draft. **Ali Hasan Ali:** Writing – review & editing, Methodology, Software, Validation, Visualization, Project administration.

Declaration of competing interest

The authors declare that they have no known competing financial interests or personal relationships that could have appeared to influence the work reported in this paper.

Acknowledgment

The authors extend their appreciation to the Deanship of Research and Graduate Studies at King Khalid University for funding this work through Large Research Project under grant number RGP2/525/45.

References

[1] Amjad M, Iffat Zehra S, Nadeem NA, Saleem A, Issakhov A. Influence of Lorentz force and induced magnetic field effects on Casson micropolar nanofluid flow over a permeable curved stretching/shrinking surface under the stagnation region. Surf Interfaces 2020;21:100766.
[2] Sadiq MA, Hayat T. Entropy optimized flow of Reiner-Rivlin nanofluid with chemical reaction subject to stretchable rotating disk. Alex Eng J 2021.
[3] Loganathan K, Mohana K, Mohanraj M, Sakthivel P, Rajan S. Impact of third-grade nanofluid flow across a convective surface in the presence of inclined Lorentz force: an approach to entropy optimization. J Therm Anal Calorim 2021;144(5).
[4] Choi, S. US, and Jeffrey A. Eastman. *Enhancing thermal conductivity of fluids with nanoparticles*. No. ANL/MSD/CP-84938; CONF-951135-29. Argonne National Lab., IL (United States), 1995.
[5] Muhammad T, Waqas H, Khan SA, Ellahi R, Sait SM. Significance of nonlinear thermal radiation in 3D Eyring-Powell nanofluid flow with Arrhenius activation energy. J Therm Anal Calorim 2021;143(2):929–44.
[6] Wang Na, Maleki A, Nazari MA, Tlili I, Shadloo MS. Thermal conductivity modeling of nanofluids contain MgO particles by employing different approaches. Symmetry 2020;12(2):206.
[7] Hayat AU, Ullah I, Khan H, Weera W, Galal AM. Numerical simulation of entropy optimization in radiative hybrid nanofluid flow in a variable features darcy-forchheimer curved surface. Symmetry 2022;14(10):2057.
[8] Ullah I. Activation energy with exothermic/endothermic reaction and Coriolis force effects on magnetized nanomaterials flow through Darcy-Forchheimer porous space with variable features. Waves Random Complex Media 2022:1–14.
[9] Mebarek-Oudina F. "Convective heat transfer of Titania nanofluids of different base fluids in cylindrical annulus with discrete heat source". Heat Transfer—Asian Research 2019;48(1):135–47.
[10] Reddy YD, Fateh Mebarek-Oudina B, Goud S, Is"Radiation AI. Velocity and thermal slips effect toward MHD boundary layer flow through heat and mass transport of williamson nanofluid with porous medium.". Arab J Sci Eng 2022:1–15.
[11] Maleki A, Elahi M, El Haj M, Assad MA, Nazari MS, Shadloo, Nabipour Narjes. Thermal conductivity modeling of nanofluids with ZnO particles by using approaches based on artificial neural network and MARS. J Therm Anal Calorim 2021;143(6):4261–72.
[12] Shahrestani I, Misagh AM, Shadloo MS, Tlili I. Numerical investigation of forced convective heat transfer and performance evaluation criterion of Al2O3/water nanofluid flow inside an axisymmetric microchannel. Symmetry 2020;12(1):120.
[13] Ramezanizadeh M, Ahmadi MA, Ahmadi MH, Nazari MA. Rigorous smart model for predicting dynamic viscosity of Al 2 O 3/water nanofluid. J Therm Anal Calorim 2019;137(1):307–16.
[14] Khan SU, Rauf A, Shehzad SA, Abbas Z, Javed T. Study of bioconvection flow in Oldroyd-B nanofluid with motile organisms and effective Prandtl approach. Phys A 2019;527:121179.
[15] Senthil K, Kalainathan S, Ruban Kumar A. Bulk size crystal growth, spectral, optical, luminescence, thermal, mechanical, and dielectric properties of organic single crystal. J Therm Anal Calorim 2014;118(1):323–31.
[16] Ullah I, Alajlani Y, Pasha AA, Adil M, Weera W. Theoretical investigation of hybrid nanomaterials transient flow through variable feature of Darcy-Forchheimer space with exponential heat source and slip condition. Sci Rep 2022;12(1):1–14.
[17] Patel H, Mittal A, Nagar T. Effect of magnetic field on unsteady mixed convection micropolar nanofluid flow in the presence of non-uniform heat source/sink. Int J Ambient Energy 2024;45(1):2266748.
[18] Patel H, Mittal A, Nagar T. Fractional order simulation for unsteady MHD nanofluid flow in porous medium with Soret and heat generation effects. Heat Transfer 2023;52(1):563–84.
[19] Patel HR, Mittal AS, Darji RR. MHD flow of micropolar nanofluid over a stretching/shrinking sheet considering radiation. Int Commun Heat Mass Transfer 2019;108:104322.
[20] Mittal AS, Kataria HR. Three dimensional CuO–Water nanofluid flow considering Brownian motion in presence of radiation. Karbala Int J Mod Sci 2018;4(3):275–86.

[21] Kataria HR, Mittal AS. Velocity, mass and temperature analysis of gravity-driven convection nanofluid flow past an oscillating vertical plate in the presence of magnetic field in a porous medium. Appl Therm Eng 2017;110:864–74.
[22] Hussein SA, Ahmed SE, Arafa AA. Numerical treatment of thermal and concentration convection along with induced magnetic field on peristaltic pumping of a magnetic six-constant Jeffrey nanofluid through a vertical divergent channel. Numerical Heat Transfer, Part a: Applications 2023;84(8):877–904.
[23] Kataria HR, Mittal AS. Analysis of casson nanofluid flow in presence of magnetic field and radiation. Math Today 2017;33(1):99–120.
[24] Kataria HR, Mittal AS. Mathematical model for velocity and temperature of gravity-driven convective optically thick nanofluid flow past an oscillating vertical plate in presence of magnetic field and radiation. J Nigerian Math Soc 2015;34(3):303–17.
[25] Sheikholeslami M, Kataria HR, Mittal AS. Radiation effects on heat transfer of three dimensional nanofluid flow considering thermal interfacial resistance and micro mixing in suspensions. Chin J Phys 2017;55(6):2254–72.
[26] Li Z, Sheikholeslami M, Mittal AS, Shafee A, Haq R-u. "Nanofluid heat transfer in a porous duct in the presence of Lorentz forces using the lattice Boltzmann method". The European Physical Journal plus 2019;134:1–10.
[27] Sheikholeslami M, Kataria HR, Mittal AS. Effect of thermal diffusion and heat-generation on MHD nanofluid flow past an oscillating vertical plate through porous medium. J Mol Liq 2018;257:12–25.
[28] Karbala International Journal of Modern Science 4 (3), 275-286.
[29] Dogonchi AS, Waqas M, Seyyedi SM, Hashemi-Tilehnoee M, Ganji DD. A modified Fourier approach for analysis of nanofluid heat generation within a semi-circular enclosure subjected to MFD viscosity. Int Commun Heat Mass Transfer 2020;111:104430.
[30] Ullah I. Heat transfer enhancement in Marangoni convection and nonlinear radiative flow of gasoline oil conveying Boehmite alumina and aluminum alloy nanoparticles. Int Commun Heat Mass Transfer 2022;132:105920.
[31] Hamid A, Khan M. Impacts of binary chemical reaction with activation energy on unsteady flow of magneto-Williamson nanofluid. J Mol Liq 2018;262:435–42.
[32] Bestman AR. Natural convection boundary layer with suction and mass transfer in a porous medium. Int J Energy Res 1990;14(4):389–96.
[33] Awad FG, Motsa S, Khumalo M. Heat and mass transfer in unsteady rotating fluid flow with binary chemical reaction and activation energy. PLoS One 2014;9(9):e107622.
[34] Ullah Zakir, Ullah Ikram, Zaman Gul, Sun Tian Chuan. "A numerical approach to interpret melting and activation energy phenomenon on the magnetized transient flow of Prandtl–Eyring fluid with the application of Cattaneo–Christov theory". *Waves Random Complex Media* (2022) 1-21 Flow" *Scientific Reports* 2020;10(1):1–16.
[35] Hayat T, Ullah Ikram, Alsaedi A, Asghar Saleem. Importance of activation energy and heat source on nanoliquid flow with gyrotactic microorganisms. Sci Iran 2020;27(6):3381–9.
[36] Ullah I, Ali R, Nawab H, Uddin I, Muhammad T, Khan I, et al. Theoretical analysis of activation energy effect on prandtl-eyring nanoliquid flow subject to melting condition. J Non-Equilib Thermodyn 2022;47(1):1–12.
[37] Ullah I, Refat Ullah MS, Alqarni W-F, Muhammad T. Combined heat source and zero mass flux features on magnetized nanofluid flow by radial disk with the applications of coriolis force and activation energy. Int Commun Heat Mass Transfer 2021;126:105416.
[38] Bejan, Adrian. "A study of entropy generation in fundamental convective heat transfer." (1979): 718-725.
[39] Alkanhal TA, Sheikholeslami M, Arabkoohsar A, Haq R-u, Shafee A, Li Z, et al. Simulation of convection heat transfer of magnetic nanoparticles including entropy generation using CVFEM. Int J Heat Mass Transf 2019;136:146–56.
[40] Li Z, Sheikholeslami M, Jafaryar M, Shafee A, Chamkha AJ. Investigation of nanofluid entropy generation in a heat exchanger with helical twisted tapes. J Mol Liq 2018;266:797–805.
[41] Cengel YA, Boles MA, Kanoglu M. Thermodynamics: an engineering approach. New York: McGraw-hill; 2011.
[42] Dormohammadi R, Farzaneh-Gord M, Ebrahimi-Moghadam A, Ahmadi MH. Heat transfer and entropy generation of the nanofluid flow inside sinusoidal wavy channels. J Mol Liq 2018;269:229–40.
[43] Rashidi MM, Bagheri S, Momoniat E, Freidoonimehr N. Entropy analysis of convective MHD flow of third grade non-Newtonian fluid over a stretching sheet. Ain Shams Eng J 2017;8(1):77–85.
[44] Tayebi Tahar, Dogonchi AS, Chamkha Ali J, Hamida Mohamed Bechir Ben, El-Sapa Shreen, Galal Ahmed M. "Micropolar nanofluid thermal free convection and entropy generation through an inclined I-shaped enclosure with two hot cylinders". *Case Studies in Thermal Engineering* 2022:101813.
[45] Sadiq MA, Hayat T. Entropy optimized flow of Reiner-Rivlin nanofluid with chemical reaction subject to stretchable rotating disk. Alex Eng J 2022;61(5):3501–10.
[46] Basit MA, Farooq U, Imran M, Fatima N, Alhushaybari A, Noreen S, et al. Comprehensive investigations of (Au-Ag/Blood and Cu-Fe3O4/Blood) hybrid nanofluid over two rotating disks: numerical and computational approach. Alex Eng J 2023;72:19–36.
[47] Ullah I, Jan RU, Khan H, Alam MM. Improving the thermal performance of (ZnO-Ni/H2O) hybrid nanofluid flow over a rotating system: the applications of Darcy Forchheimer theory. Waves Random Complex Media 2022:1–17.

Refat Ullah Jan Ph.D. scholar at the Department of Mathematics Islamia College Peshawar KP, Pakistan. He received M.S degree in Mathematics from Qurtuba University of Science and Technology Peshawar, KP, Pakistan

Dr. Ikram Ullah is currently working as an Assistant Professor at Department of Natural Sciences and Humanities, University of Engineering and Technology, Mardan. 23200, Pakistan. He received his PhD degree from Department of Mathematics at Quaid-i-Azam University, Pakistan. He received his M.Phil degrees from Quaid-i-Azam University. His research interests include nanomaterials, hybrid nanomaterials, entropy analysis and heat mass transfer.

Dr. Mohammad Mehtab Alam is currently working as an Assistant Professor at Department of Basic Medical Sciences, College of Applied Medical Science, King Khalid University, Abha 61421, Saudi Arabia

Ali Hasan Ali is a dedicated researcher at the Institute of Mathematics, University of Debrecen, Hungary. He holds a B. Sc. Ed. in Mathematics from University of Mosul, Iraq, and an M.Sc. in Applied Mathematics from Wright State University, USA, and a Ph.D. in Mathematics from University of Debrecen, Hungary. Ali's research interests include Applied Mathematics, Modelling, Optimization, Fractional Calculus, Computational Mathematics, and Approximation. He has published over 50 research papers in Scopus/WOS-indexed journals in esteemed publishers, including Elsevier, Springer, Wiley, Taylor and Francis, and IEEE. In addition to his research, Ali actively contributes to the academic community as a reviewer for prestigious journals and has served as the Program Committee Chair and member for numerous international conferences.